Possibility of detecting forest fires from space during daytime under conditions of broken clouds. Part 1

V.G. Astafurov

Institute of Atmospheric Optics,
Siberian Branch of the Russian Academy of Sciences, Tomsk
Tomsk State University of Control Systems and Radioelectronics

Received January 5, 2000

The efficiency of daytime detection of flaming zones from space by thermal radiation is limited by the noise produced by solar radiation reflected in the "cloudy atmosphere – underlying surface" system. In this paper, the Monte Carlo method is applied to the study of statistical characteristics of solar and thermal radiation noise measured with a radiometer. The algorithm for numerical simulation is presented. The efficiency of the flaming zones detection depending on their size and cloud amount is estimated by the value of the signal-to-noise ratio. The mean thermal radiation noise is compared with the solar radiation noise.

Introduction

Detection of the Earth's surface areas with high-temperature anomalies from space is based on measurements of IR radiation in the spectral regions from 3.55 to 3.93 and from 10.3 to 11.3 μm, which lie in the atmospheric transmission windows. These are the regions employed as the third and fourth NOAA AVHRR spectral channels.[1] The possibility of night-time detection of forest fires under conditions of broken clouds was considered in Refs. 2 and 3. At night, the main distorting factor is clouds, which partially or fully cover the flaming zone. Based on the results obtained, a statistical model was proposed for describing fluctuations in the radiation power measured with a radiometer. This radiation includes the thermal radiation from a flaming zone and the background radiation, which, in turn, includes the IR radiation from the Earth's surface, atmosphere, and clouds. The probability of detecting a fire was calculated based on the Neumann – Pearson criterion.

In Ref. 4 it was noted that the efficiency of detecting a fire is determined by two factors, *viz.*, by the periodicity of observations and by the capability of detecting a small fire. For an ideal detector, the mean duration of a fire before its detection t_m is

$$\langle t_m \rangle \approx (1.04)^{m-1} \langle t_1 \rangle / m ,$$

where m is the periodicity of observations; $\langle t_m \rangle$ and $\langle t_1 \rangle$ are the mean duration of a fire before its detection at the periodicity of m and 1 times a day, $\langle t_1 \rangle \approx 4.5$–$6.1$ h. Higher periodicity is connected with invoking space information obtained in daytime. In this case, the efficiency of fire detection decreases because of the additional noise in the spectral region of 3.55–3.93 μm. This noise is caused by the solar radiation reflected in the "cloudy atmosphere – surface" system and the value of this noise is also significant.[5] In this paper, which continues the studies of Refs. 2 and 3, the statistical characteristics of solar component of the background are considered and the efficiency of daytime fire detection from space is evaluated based on the obtained results.

Statement of the problem and method of solution

Figure 1 shows the scheme of fire detection with an IR radiometer having the field-of-view angle Ω_R and located at the altitude H_R. The solar radiation is incident on the atmospheric top (plane $z = H^*$) along the direction of a unit vector $\boldsymbol{\omega}_0$.

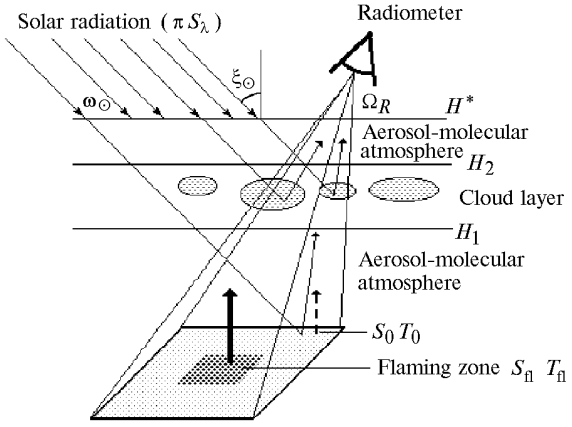

Fig. 1. Scheme of fire detection.

Here πS_λ is the spectral solar constant, and ξ_0 is the solar zenith angle. The total power measured with a radiometer is

0235-6880/00/04 326-05 $02.00

$$p(\mathbf{r}_R, \boldsymbol{\omega}_R, \Delta\lambda) = \int\limits_{\Omega_R} d\boldsymbol{\omega} \int\limits_{S_R^*} d\boldsymbol{\rho} \int\limits_{\Delta\lambda} d\lambda\, k(\lambda)\, I(\boldsymbol{\rho}, \boldsymbol{\omega}, \lambda)\,,$$

where the vector $\mathbf{r}_R$ determines the position of the radiometer; the unit vector $\boldsymbol{\omega}_R$ gives the radiometer's sighting direction; S_R^* is the surface of the receiving aperture; $\Delta\lambda$ is the spectral region; $k(\lambda)$ is the optical filter transmittance at the wavelength λ; $I(\boldsymbol{\rho}, \boldsymbol{\omega}, \lambda)$ is the intensity at the point $\boldsymbol{\rho} \in S_R^*$ in the direction of the unit vector $\boldsymbol{\omega} = (a, b, c)$ at the wavelength λ. If the changes in the intensity at the surface of the receiving aperture are ignored, then

$$p(\mathbf{r}_R, \boldsymbol{\omega}_R, \Delta\lambda) \approx S_R \int\limits_{\Omega_R} d\boldsymbol{\omega} \int\limits_{\Delta\lambda} d\lambda\, k(\lambda)\, I(\mathbf{r}_R, \boldsymbol{\omega}, \lambda), \quad (1)$$

where S_R is the effective area of the receiving aperture.

Under the conditions of broken clouds, the main sources of radiation fluctuations are fluctuations of the extinction coefficient $\sigma(\mathbf{r})$ due to the stochastic geometry of a cloud field. The study of statistical characteristics of the total radiation power measured with a radiometer is based on the stochastic equation of transfer

$$\mathbf{T}\cdot\nabla I(\mathbf{r}, \mathbf{T}) + \sigma(\mathbf{r})\, I(\mathbf{r}, \mathbf{T}) = \sigma(\mathbf{r})\, \Lambda(\mathbf{r}) \times$$
$$\times \int\limits_{4\pi} g(\mathbf{r}, \mathbf{T}, \mathbf{T}')\, I(\mathbf{r}, \mathbf{T}')\, d\mathbf{T}' + \sigma(\mathbf{r})\, J(\mathbf{r}, \mathbf{T})\,, \quad (2)$$

where $J(\mathbf{r}, \boldsymbol{\omega})$ is the source function, which is isotropic and equals to

$$J(\mathbf{r}, \mathbf{T}) = [1 - \Lambda(\mathbf{r})]\, B_\lambda[T(z)]$$

provided that the conditions of local thermodynamic equilibrium are fulfilled. Here $B_\lambda[T(z)] = 2hc^2 / [\lambda^5(\exp(hc/\lambda kT) - 1)]$ is the Planck's function, h is the Planck's constant, and k is the Boltzmann constant. The boundary conditions of Eq. (2) have the form

$$I(\mathbf{r}_H, \mathbf{T}) = \pi S_\lambda\, \delta(\mathbf{T} - \mathbf{T}_0)\,, \quad \mu < 0 \quad (3)$$

in the plane $z = H^*$;

$$I(\mathbf{r}_0, \mathbf{T}) = \varepsilon_\lambda\, B_\lambda(T_s(x, y)) +$$
$$+ \frac{1 - \varepsilon_\lambda}{\pi} \int\limits_{2\pi^-} I(\mathbf{r}_0, \mathbf{T}')\, |\mu'|\, d\mathbf{T}'\,, \quad \mu > 0 \quad (4)$$

in the underlying surface, which is isotropically emitting and isotropically reflecting (Lambertian). In Eqs. (3) and (4) the following designations are used: $\mathbf{r}_0 = (x, y, 0)$, $\mathbf{r}_H = (x, y, H^*)$; $\mu = c = \cos(\psi)$; ψ is the angle between the axis OZ and the unit vector $\boldsymbol{\omega}$; ε_λ is the relative emittance of the surface at the wavelength λ; $2\pi^-$ means that the integral in Eq. (4) is calculated over the lower hemisphere ($\mu < 0$); $T_s(x, y)$ is the surface temperature at the point (x, y); $\sigma(\mathbf{r})$ and $\Lambda(\mathbf{r})$ are the extinction coefficient and the single-scattering albedo at the point $\mathbf{r}$; $\delta(\boldsymbol{\omega} - \boldsymbol{\omega}_0)$ is the Dirac delta function.

To estimate the statistical characteristics of the noise of solar radiation p_S, the solar and thermal radiation $p_S + p_{IR}$, and background and flaming zone radiation $p = p_S + p_{IR} + p_{fl}$, we used the method of numerical simulation of cloud fields and radiation.[6] Toward this end, realizations of the cloud field were simulated, and for each of them we determined p_S and $p_{IR} + p_{fl}$. Then moments and power histograms were calculated by statistical processing of the obtained results.

Let us consider a plane-parallel model of the atmosphere, which is horizontally homogeneous (except for the cloud layer), to be in the local thermodynamic equilibrium, and has the temperature $T(z)$ at the altitude z and the net coefficient of aerosol and gas extinction $\sigma_\Sigma(z, \lambda)$. The cloud layer is bounded by the altitude interval $[H_1, H_2]$. The cloud extinction and scattering coefficients are significantly larger than the corresponding characteristics of aerosol and molecular scattering. Therefore, within the cloud layer we take into account only radiation interaction with the cloud matter,[6,7] i.e., we assume $\sigma_\Sigma(z, \lambda) = 0$ at $z \in [H_1, H_2]$. Thus,

$$\sigma(\mathbf{r}) = \begin{cases} \sigma_c(\mathbf{r}), & z \in [H_1, H_2], \\ \sigma_\Sigma(z), & z \notin [H_1, H_2], \end{cases}$$

where $\sigma_c(\mathbf{r})$ is the cloud extinction coefficient.

Let us define the term "broken clouds"[6] as a cumulus field with the stochastic geometry and deterministic inner structure. The optical model of clouds in the interval $[H_1, H_2]$ is given in the form of scalar fields of the cloud extinction coefficient $\sigma_c(\mathbf{r}) = \sigma_c\, \chi(\mathbf{r})$, single-scattering albedo $\Lambda_c\, \chi(\mathbf{r})$, and scattering phase function $g(\boldsymbol{\omega}, \boldsymbol{\omega}')\, \chi(\mathbf{r})$, where $\chi(\mathbf{r})$ is the indicator field, $\chi(\mathbf{r}) = 1$ at $\mathbf{r} \in \Theta$ and $\chi(\mathbf{r}) = 0$ at $\mathbf{r} \notin \Theta$; Θ is a random set of points at which the cloud matter with the extinction coefficient σ_c is present. Hereinafter, the obvious dependence on the wavelength λ is omitted.

Recall that, as in Ref. 2, realizations of the cloud field are generated with the use of the Poisson flow of points $\{(x_c, y_c)\}$, which determine the position of cloud centers, at the plane $z = H_1$. Clouds have the shape of a truncated paraboloid of revolution

$$z = D - \frac{4}{D}\,[(x - x_c)^2 - (y - y_c)^2]\,,$$

whose base diameter D is equal to the height and has the exponential probability density $f(D) \sim \exp(-\alpha D)$, $30 < D < 1200$ m. The cloud amount N is related to the mean number of cloud centers ν per unit area of the plane $z = H_1$ as[8]:

$$N = 1 - \exp(-\nu \overline{D^2}\, /4)\,,$$

where $\overline{D^2} = \int_{D_{\min}}^{D_{\max}} D^2 f(D)\, dD$.

Taking into account that the transfer equation (2) is linear, we seek for its solution at a given realization of the cloud field in the form

$$I(\mathbf{r}, \mathbf{T}) = I_\Sigma(\mathbf{r}, \mathbf{T}) + I_S(\mathbf{r}, \mathbf{T}),$$

where $I_\Sigma(\mathbf{r}, \boldsymbol{\omega})$ and $I_S(\mathbf{r}, \boldsymbol{\omega})$ are the intensity of the upwelling thermal radiation, including the flaming zone radiation, and the intensity of the solar radiation scattered by the "cloudy atmosphere – surface" system. When determining the intensity of thermal radiation, we ignore its scattering and reflection from the surface, i.e., we assume that in Eq. (2) $\Lambda(\mathbf{r}) = 0$ and the boundary condition (4) for $z = 0$ has the form $I_\Sigma(\mathbf{r}_0, \boldsymbol{\omega}) = \varepsilon_\lambda B_\lambda [T_s(x, y)]$, $\mu > 0$. The latter approximation is caused by the fact that in the atmospheric transmission windows the contribution of the downwelling atmospheric radiation reflected by the surface and attenuated by the above atmospheric column is negligibly small,[5] because the Earth's surface emits in the thermal region of the spectrum as a black body. According to Ref. 9, the emittance is $\varepsilon_\lambda \approx 0.9$–$0.98$. At the atmospheric top $I_\Sigma(\mathbf{r}_H, \boldsymbol{\omega}) = 0$ at $\mu < 0$. With the allowance made for this,[2] we have

$$I_\Sigma(\mathbf{r}_R, \mathbf{T}) = \varepsilon_\lambda B_\lambda [T_s(x_0, y_0)] \exp\left(-\int_{t_H}^{t_0} \sigma(\mathbf{r}_R - \mathbf{T}t)dt\right) +$$

$$+ \int_{t_H}^{t_0} B_\lambda[T(H_R - ct)] \exp\left[-\int_{t_H}^{t} \sigma(\mathbf{r}_R - \mathbf{T}s)\, ds\right] \sigma(\mathbf{r}_R - \mathbf{T}t)dt, \quad (5)$$

where $t = t_0$ and $t = t_H$ determine the points of intersection of the straight line $\mathbf{r} = \mathbf{r}_R - \boldsymbol{\omega}t$ with the planes $z = 0$ and $z = H^*$; (x_0, y_0) are the coordinates of the point of intersection of the straight line $\mathbf{r} = \mathbf{r}_R - \boldsymbol{\omega}t$ with the plane $z = 0$. The first term in Eq. (5) is the surface radiation transformed by the atmosphere, and the second term is the atmospheric radiation.

Let us turn to consideration of the solar radiation noise, whose power $p_S(\theta, \Delta\lambda)$ is a linear functional of $I_S(\mathbf{r}, \boldsymbol{\omega})$ (θ is the angle between the vector $\boldsymbol{\omega}_R$ and the nadir direction). Its value for a given realization of the cloud field can be found by solving Eq. (2) at $J(\mathbf{r}, \boldsymbol{\omega}) = 0$, the boundary conditions (3), and

$$I_S(\mathbf{r}_0, \mathbf{T}) = \frac{1 - \varepsilon_\lambda}{\pi} \int_{2\pi} I(\mathbf{r}_0, \mathbf{T}') |\mu'|\, d\mathbf{T}', \quad \mu > 0 \quad (6)$$

for $z = 0$.

For solution of the transfer equation, the method of conjugate walk was used.[10] Trajectories are plotted from the point of observation in the direction $\boldsymbol{\omega}_0 = (\varphi_0, \psi_0)$, which is uniformly distributed within Ω_R. Here φ_0 and ψ_0 are the zenith and azimuth angles of a trajectory. For every realization of the cloud field, the sought power is estimated as $\hat{p}_S(\theta, \Delta\lambda) = S_R\, \Omega_R\, \pi\, S_\lambda\, \Delta\lambda\, \langle\gamma\rangle$, where $\langle\gamma\rangle$ is a random parameter

$$\gamma = \sum_{i=1}^{L} \frac{e^{-\tau_i}\, \eta_i\, w_i}{2\pi}, \quad (7)$$

averaged over the number of trajectories M, L is the number of collisions; τ_i is the optical length of the section from the point of the ith collision to the point at the atmospheric top along the direction $-\boldsymbol{\omega}_0$; η_i is determined as $\eta_i = g[\mathbf{r}_i, (\boldsymbol{\omega}_{i-1}, -\boldsymbol{\omega}_0)]$ if the ith collision occurs in the cloud layer, and $\eta_i = 2 \cos \xi_0$ if a photon fell on the surface; w_i is the weight of a photon after the ith collision; $\mathbf{r}_i = (x_i, y_i, z_i)$ is the radius vector of the point of the ith collision. The initial weight of a photon

$$w_0 = \begin{cases} T(\Delta\lambda, |\mu_0|) \exp[-(\tau_{a1}(\Delta\lambda) + \tau_{a2}(\Delta\lambda)/|\mu_0|)], \mathbf{r}_1 \in \Sigma, \\ T_1(\Delta\lambda, |\mu_0|) \exp[-(\tau_{a1}(\Delta\lambda))/|\mu_0|], \mathbf{r}_1 \in \Theta, \end{cases}$$

where $T(\Delta\lambda, |\mu_0|)$ and $T_1(\Delta\lambda, |\mu_0|)$ are the mean molecular transmittance of the entire atmosphere and the over-cloud layer in the spectral interval $\Delta\lambda$ along the direction characterized by the zenith angle ψ_0 ($\mu_0 = \cos(\psi_0)$); $\tau_{ak}(\Delta\lambda/|\mu_0|)$ is the mean aerosol optical depth of the kth layer in the spectral interval $\Delta\lambda$; Σ is the set of surface points. In the case of scattering in the cloud layer $w_i = w_{i-1}\, \Lambda_c$, and in the case of reflection from the surface $w_i = w_{i-1}(1 - \varepsilon_\lambda)$. As for the thermal radiation, the effects of scattering in the over-cloud ($k = 1$) and under-cloud ($k = 2$) layers are neglected, i.e., for them $\Lambda = 0$. The event that the photon trajectory intersects the under-cloud layer is taken into account by multiplying the photon weight by $T_2(\Delta\lambda, |\mu|) \exp(-\tau_{a2}(\lambda)/|\mu|)$, where $\mu = \cos\psi$, and ψ is the zenith angle of the trajectory. Note that if a photon from the cloud layer or after its reflection from the surface arrives at the over-cloud layer, then its trajectory terminates. Let the point of the ith photon collision be denoted as $\mathbf{r}_i$. Determination of the mean free path and τ_i in Eq. (7) within the cloud layer is connected with calculation of the total length of the sections of the straight lines $\mathbf{r} = \mathbf{r}_i + \boldsymbol{\omega}_i t$ or $\mathbf{r} = \mathbf{r}_i - \boldsymbol{\omega}_0 t$ lying inside the cloud layer. Recall that the shape of a cloud is a truncated paraboloid of revolution. If the cross section of the cloud field by the plane perpendicular to the plane XOY comes through the photon trajectory, then the problem is reduced to calculation of the lengths of the sections being inside the parabolas, i.e., to solution of quadratics.

Calculated results and discussion

In our calculations, we took the following values of the parameters: radiometer altitude H_R = 850 km, Ω_R = 1.88 10^{-6} sr, sighting angle θ = 0. We considered the simplest model of a flaming zone having the temperature T_{fl} = 1000 K and the area S_{fl} (Fig. 1). The surface temperature beyond the flaming zone was T_0 = 300 K. The spectral interval in the calculations was divided into three sub-intervals, *viz.*, 3.55–3.6, 3.6–3.8, and 3.8–3.93 μm, based on the available information on the spectral dependence of the aerosol extinction coefficients.[11] The program for calculating the mean transmittance of the over-cloud and under-cloud layers in the selected spectral intervals with regard for the zenith angle dependence was kindly put at my disposal by K.M. Firsov. The meteorological model of mid-latitude summer was used.[12] The presented results were obtained for the spectral sub-interval of 3.6–3.8 μm. The altitude of the cloud base was H_1 = 1 km, and the values of σ_c and Λ_c corresponded to C_1 cloud model[13] and were equal to 20.28 km^{-1} and 0.94.

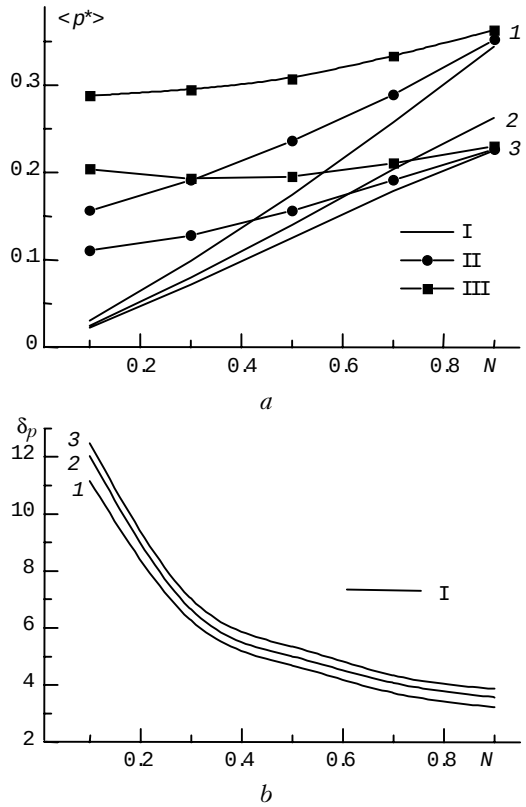

Fig. 2. Normalized mean power of solar radiation noise $<p_S^*>$ (*a*) and its relative rms. deviation δ_p (*b*) vs. cloud amount *N*: ξ_υ = 10° (*1*), 30° (*2*), and 40° (*3*); $(1 - \varepsilon_\lambda)$ = 0 (I), 0.1 (II), and 0.2 (III).

Figures 2 and 3 show the calculated statistical characteristics of the normalized power $p^* = p_S(\theta, \Delta\lambda)/\pi S_\lambda \Omega_R S_R \Delta\lambda$ of the solar radiation reflected by the "cloudy atmosphere – surface" system. It is worthy to note an essential dependence of the mean power on the surface reflection coefficient $(1 - \varepsilon_\lambda)$. For a rather large value $(1 - \varepsilon_\lambda)$ = 0.2, the dependence of the mean power on the cloud amount *N* (Fig. 2*a*) becomes insignificant (curves marked by squares), because the passage of solar radiation through gaps between clouds is compensated for by its reflection from the surface.

The decrease of $<p^*>$ with the increase of the solar zenith angle is explained by the increasing effect of cloud lateral surfaces and their scattering phase function. Therefore, based on the value of the solar radiation noise, at sensing along nadir, large solar zenith angles are preferable for fire detection.

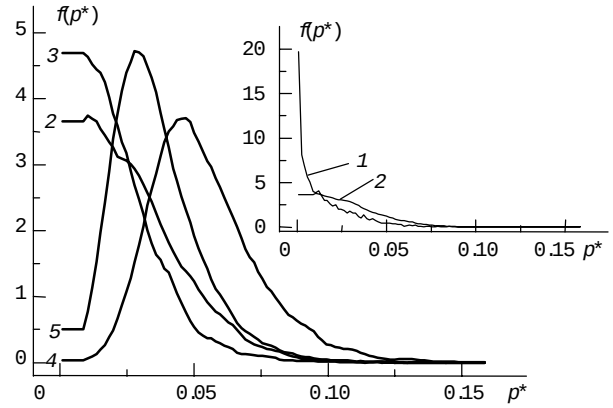

Fig. 3. Histograms of normalized power of solar radiation noise: *N* = 0.3 and ξ_υ = 5° (*1*); *N* = 0.5 and ξ_υ = 5° (*2*); *N* = 0.5 and $\xi\upsilon$ = 40° (*3*); *N* = 0.9 and $\xi\upsilon$ = 5° (*4*); *N* = 0.9 and $\xi\upsilon$ = 40° (*5*).

The calculated results show that the increase of the surface reflection coefficient has practically no effect on the value of the relative rms deviation $\delta_p = \sqrt{D(p_S)}/<p_S>$ of the power of solar radiation noise, because the level of fluctuations of the solar radiation scattered by clouds is mostly determined by the stochastic geometry of the cloud layer. Figure 2*b* shows the dependence of δ_p on *N* at $(1 - \varepsilon_\lambda)$ = 0. Note that the relative error in the calculated p_S moments does not exceed 4%. The histograms shown in Fig. 3 illustrate their significant dependence not only on the cloud amount, but also on the solar zenith angle. The histograms were calculated for a surface not reflecting solar radiation (ε_λ = 1).

The efficiency of fire detection under conditions of a cloudy atmosphere can be indirectly judged from the signal-to-noise ratio denoted here as *SNR*. In our case, $SNR = <p_{fl}>/\sqrt{D(p)}$ is the ratio of the mean power of the flaming zone radiation $<p_{fl}>$ to the rms deviation $\sqrt{D(p)}$ of the total power *p* measured with the radiometer. The dependence of the signal-to-noise ratio on the cloud amount is shown in Fig. 4 for flaming zones having the area S_{fl} = 100 and 400 m^2. It is seen from the results presented that the appearance of solar radiation noise significantly decreases the *SNR*. As a result, for the flaming zone with S_{fl} = = 100 m^2 the signal-to-noise ratio does not exceed 0.5,

whereas in the case of no solar radiation $SNR \approx 1.9$ at $N = 0.1$.

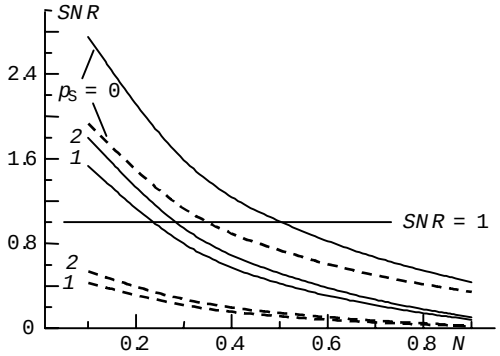

Fig. 4. Signal-to-noise ratio vs. cloud amount N: $\xi_{\upsilon} = 10°$ (*1*) and 40° (*2*); $S_{fl} = 400$ m^2 (solid curves) and 100 m^2 (dashed curves).

Let us introduce the ratios: $Q_1 = \langle p_{IR} \rangle / \langle p_S \rangle$ and $Q_2 = \langle p_{fl} \rangle / \langle p_S + p_{IR} \rangle$. The former determines the mean power ratio between the solar radiation noise and the thermal radiation noise, while the latter determines the mean power ratio between the flaming zone radiation and the net background radiation.

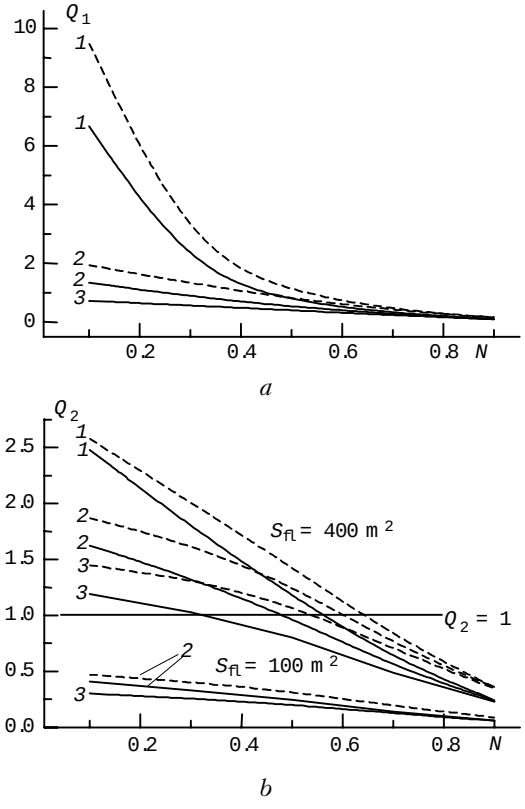

Fig. 5. Ratios Q_1 (*a*) and Q_2 (*b*) vs. cloud amount N: $1 - \varepsilon_\lambda = 0$ (*1*), 0.1 (*2*), and 0.2 (*3*); $\xi_{\upsilon} = 10°$ (solid curves) and 40° (dashed curves).

The calculated results on Q_1 and Q_2 are shown in Fig. 5. The level of solar radiation noise under conditions of a cloudy atmosphere and the reflecting surface is close to the thermal radiation noise (curves *2* and *3* in Fig. 5*a*). At the cloud amount $N < 0.3$, the ratio Q_1 decreases by 2.5 to 4 times as ε_λ increases from 0.9 to 1. This is connected with the large contribution of solar radiation reflected from the surface at $N < 0.3$. Since the emittance $\varepsilon_\lambda > 0.9$ for most types of the surfaces, its value, along with the cloud amount, should be taken into account in determining the fire detection threshold by the Neumann – Pearson criterion.[2] Because of a significant level of the solar radiation noise, the ratio Q_2 does not exceed 0.5 for the flaming zone with the area $S_{fl} = 100$ m^2 (Fig. 5*b*). On the other hand, the relative level of fluctuations of the solar radiation noise at small cloud amount is rather high, for example, at $N = 0.1$ $\delta_p > 10$ (see Fig. 2*b*). Therefore, the efficiency of detecting small flaming zones at small cloud amount is low. However, the mean power for the flaming zone with $S_{fl} = 400$ m^2 at $N < 0.5$ exceeds the mean power of the total noise, what makes it possible to detect such flaming zones.

The obtained results indirectly characterize the possibility of detecting flaming zones under daytime conditions. The most complete information on the possibilities of detecting fires can be obtained from a closed numerical experiment, as it was done for the night conditions in Ref. 3.

References

1. L. Lauritson, G.J. Nelson, and F.W. Porto, *Data Extraction and Calibration of "Tiros-N"/NOAA Radiometers. NESS-107. Technical Memorandum* (Washington, 1979), 58 pp.
2. V.G. Astafurov and G.A. Titov, Atmos. Oceanic Opt. **9**, No. 5, 409–414 (1996).
3. V.G. Astafurov, Atmos. Oceanic Opt. **12**, No. 3, 251–256 (1999).
4. G.N. Korovin, S.A. Bartalev, and A.I. Belyev, Lesnoe Khozyaistvo, No. 4, 45–48 (1998).
5. M.S. Malkevich, *Optical Study of the Atmosphere from Satellite* (Nauka, Moscow, 1973), 303 pp.
6. V.E. Zuev and G.A. Titov, Atmos. Oceanic. Opt. **8**, Nos. 1–2, 105–115 (1995).
7. J. Lenoble, *Radiative Transfer in Scattering and Absorbing Atmospheres. Standard Methods of Calculation* (Gidrometeoizdat, Leningrad, 1990), 264 pp.
8. O.A. Avaste, in: *Radiation and Cloudiness* (IAiFA AN ESSR, Tartu, 1969), pp. 98–117.
9. K.Ya. Kondrat'ev, *Radiative Characteristics of the Earth's Atmosphere* (Gidrometeoizdat, Leningrad, 1969), 564 pp.
10. B.A. Kargin, *Statistical Simulation of the Field of Solar Radiation in the Atmosphere* (Computer Center SB AS USSR, Novosibirsk, 1990), 206 pp.
11. G.M. Krekov and R.F. Rakhimov, *Optical Models of Atmospheric Aerosol* (Tomsk Affiliate SB AS USSR, Tomsk, 1986), 294 pp.
12. V.E. Zuev and V.S. Komarov, *Statistical Models of Temperature and Gaseous Constituents of the Atmosphere* (Gidrometeoizdat, Leningrad, 1986), 264 pp.
13. D. Deirmendjian, *Electromagnetic Waves Scattering on Spherical Polydispersions* (American Elsevier, New York, 1969).